

Research Paper

Time-dependent progress of lower urinary tract dysfunction in streptozotocin-induced diabetic rats with or without low-dose insulin treatment

Nailong Cao^{1,2#}, Rong Lv^{1#}, Daisuke Gotoh², Eduardo C. Alexandre², Naoki Yoshimura², Baojun Gu¹

1. Department of Urology, Shanghai Sixth People's Hospital Affiliated to Shanghai Jiao Tong University School of Medicine, Shanghai, China.
2. Department of Urology, University of Pittsburgh School of Medicine, Pittsburgh, Pennsylvania, USA.

These two authors contributed equally to this study.

✉ Corresponding authors: Baojun Gu, PhD, Department of Urology, Shanghai Sixth People's Hospital Affiliated to Shanghai Jiao Tong University School of Medicine 600 Yishan Road, Shanghai 200233, China. E-mail: gubaojun@yahoo.com; Naoki Yoshimura, MD, PhD, Department of Urology, University of Pittsburgh School of Medicine, Suite 700, Kaufmann Medical Bldg 3471 Fifth Ave, Pittsburgh, PA. E-mail: nyos@pitt.edu.

© The author(s). This is an open access article distributed under the terms of the Creative Commons Attribution License (<https://creativecommons.org/licenses/by/4.0/>). See <http://ivyspring.com/terms> for full terms and conditions.

Received: 2024.02.19; Accepted: 2024.04.18; Published: 2024.04.29

Abstract

Objectives: To examine time-dependent functional and structural changes of the lower urinary tract in streptozotocin-induced diabetic rats with or without low-dose insulin treatment and explore the pathophysiological characteristics of insulin therapy on lower urinary tract dysfunction (LUTD) caused by diabetes mellitus (DM).

Methods: Female Sprague–Dawley rats were divided into five groups: normal control (NC) group, 4 weeks insulin-treated DM (4-DI) group, 4 weeks DM (4-DM) group, 8 weeks insulin-treated DM (8-DI) group and 8 weeks DM (8-DM) group. DM was initially induced by i.p. injection of streptozotocin (65 mg/kg), and then the DI groups received subcutaneous implantation of insulin pellets under the mid dorsal skin. Voiding behavior was evaluated in metabolic cages. The function of bladder and urethra *in vivo* were evaluated by simultaneous recordings of the cystometrogram and urethral perfusion pressure (UPP) under urethane anesthesia. The function of bladder and urethra *in vitro* were tested by organ bath techniques. The morphologic changes of the bladder and urethra were investigated using Hematoxylin-Eosin and Masson's staining.

Results: Both 4- and 8-weeks diabetic rats have altered micturition patterns, including increased 12-h urine volume, urinary frequency/12 hours and voided volume. *In-vivo* urodynamics showed the EUS bursting activity duration is longer in 4-DM group and shorter in 8-DM group compared to NC group. UPP change in 8-DM were significantly lower than NC group. While none of these changes were found between DI and NC groups. Organ bath showed the response to Carbachol and EFS in bladder smooth muscle per tissue weights was decreased significantly in 4- and 8-weeks DM groups compared with insulin-treated DM or NC groups. In contrast, the contraction of urethral muscle and maximum urethral muscle contraction per gram of the tissue to EFS stimulation were significantly increased in 4- and 8-weeks DM groups. The thickness of bladder smooth muscle was time-dependently increased, but the thickness of the urethral muscle had no difference.

Conclusions: DM-induced LUTD is characterized by time-dependent functional and structural remodeling in the bladder and urethra, which shows the hypertrophy of the bladder smooth muscle, reduced urethral smooth muscle relaxation and EUS dysfunction. Low-dose insulin can protect against diuresis-induced bladder over-distention, preserve urethral relaxation and protect EUS bursting activity, which would be helpful to study the slow-onset, time-dependent progress of DM-induced LUTD.

Keywords: Diabetes Mellitus, Lower Urinary Tract Dysfunction, Insulin

Introduction

A healthy lower urinary tract (LUT) function relies on the coordination between bladder and urethra, which is regulated by the central and

peripheral nervous system [1]. Due to the intricate neural regulatory mechanisms and urinary continence-maintaining mechanism, the LUT is

susceptible to a wide range of disorders, including diabetes mellitus (DM) [2, 3]. DM-induced LUT dysfunction (LUTD) has been extensively documented, including diabetic urethral dysfunction, which is in most cases overlooked in comparison to diabetic bladder dysfunction [4, 5]. DM may initially promote urethral dysfunction characterized by increased urethral pressure during voiding, which may be attributed to the impairment of the urethra smooth muscle (USM) relaxation mechanism [4]. As the disease progresses, it can cause impairment of coordinated micturition due to dyssynergic activity of the external urethra sphincter, resulting in detrusor-sphincter dyssynergia (DSD) [5]. Therefore, similar to diabetic bladder dysfunction [6], the time-dependent changes of urethral function in DM are also existed and need further exploration and elucidation [7].

Although streptozotocin (STZ)-induced diabetic animal model has been widely used in previous studies [8, 9]. It is usually a short-term model, with diabetes symptoms peaking within a few weeks after induction. This contrasts with the chronic nature of diabetes in humans and does not fully replicate the pathological and physiological processes of human diabetes. Therefore, we employed low-dose insulin (approximately 2 units per 24 hours) treatment to maintain relatively stable glucose levels, slightly elevated within the range of 200 and 300 mg/dL (median level), and established a new animal model. Furthermore, we found that urethral function could be protected after insulin treatment compared to STZ-induced DM animal model, and it may be ascribed to inhibit the damage of nitric oxide (NO) pathway after insulin treatment. However, the time-dependent changes of the bladder and urethra have not been established in insulin-treated DM animal model.

Therefore, in this study, we established an insulin-treated DM animal model, analyzed the time-dependent functional and structural changes in the bladder and urethra, and then clarified the pathophysiological mechanism in DM and insulin-treated DM animal models.

Materials and Methods

Animal model establishment

Eighty-five adult female Sprague-Dawley rats (Hilltop Laboratory, Pittsburgh, Pennsylvania) weighing between 250 to 300 gm, were included in the study. DM was induced by a single intraperitoneal injection of STZ (65 mg/kg) freshly dissolved in sodium citrate buffer. Blood glucose levels were monitored weekly using a blood glucose meter

(Freestyle Lite, USA). Rats were considered to have DM when blood glucose reached or exceeded 300 mg/dL. Age-matched controls received a vehicle and rats with induced DM received subcutaneous implantation of LinBit insulin pellets (LinShin Canada, Ontario, Canada) under the mid dorsal skin. The release rate of insulin in the body was about 2 units per 24 hours. The aim was to maintain blood glucose levels between 200 and 300 mg/dL in insulin-treated DM rats. Female Sprague-Dawley rats were divided into five groups: normal control (NC) group, 4-week insulin-treated DM (4-DI) group, 4-week DM (4-DM) group, 8-week insulin-treated DM (8-DI) group and 8-week DM (8-DM) group. All animal experiments were conducted in accordance with the ARRIVE and NIH guidelines and approved by the Institutional Animal Care and Use Committees (IACUC) (Protocol approval #18090279). Efforts were made to minimize the suffering and the number of animals needed to obtain reliable results.

Metabolic cage study

Twenty-five of the rats ($n = 5$ per group) were housed in metabolic cages to assess their voiding behavior over a 12-hour period during the nocturnal phase (7PM to 7AM, lights off). Subsequently, all rats underwent cystometry and EUS electromyography (EUS-EMG) tests.

Cystometry and EUS electromyography with open urethra

The rats that underwent metabolic cage study ($n=5$ per group) were anesthetized with urethane (1.0 g/kg, i.p.). Bladder and urethra were exposed via a lower midline abdominal incision. a catheter (PE-50 Smiths Medical) was inserted through the top of the bladder to measure the intravesical pressure (Pves). The bladder catheter was connected to a pressure transducer and an infusion pump for cystometrogram (CMG) assessment. Physiological saline at room temperature was infused in the bladder to elicit repeat voiding responses. The infusion rate was 0.1 mL/min for the different groups. The following parameters were measured: bladder capacity, voided volume (VV), voiding efficiency (VE), inter-contraction interval (ICI), bladder compliance, maximum of Pves (Pves_{max}), EUS activity duration and EUS bursting activity duration. VV was determined by subtracting the post-void residual from the calculated bladder capacity. Bladder compliance was calculated according to the following formula: compliance = bladder capacity / (pressure at volume threshold for inducing a voiding contraction minus initial pressure at the start of saline infusion). VE was determined by the MV/bladder capacity x100. These parameters

were evaluated using a PowerLab unit and LabChart (AD Instruments, Colorado Springs, CO, USA).

To record EUS-EMG, two fine insulated silver wire electrodes (0.05-mm diameter) with exposed tips were inserted into lateral sides of the mid-urethra, targeting muscle fibers of the EUS. EUS-EMG was recorded and analyzed using PowerLab unit and Labchart (AD Instruments). EUS-EMG data were sampled at 5,000 Hz, 5–10 times the frequency of the major peaks as recommended to prevent aliasing. After the test finished, the bladder and urethra were extracted for Haematoxylin & Eosin (H&E) and Masson's staining.

In vivo functional studies with simultaneous recordings of intravesical pressure under isovolumetric conditions and urethral perfusion pressure (UPP)

The separate group of rats (n=6 per group) were anesthetized with isoflurane and urethane (1.0 g/kg, i.p.), and the bladder and ureters were exposed via a lower midline abdominal incision. The bladder neck was tied to allow functional separation of bladder and urethral activity. A PE-50 catheter (Clay Adams) was inserted into the bladder through the top of the bladder wall to record intravesical pressure, and a PE-50 catheter (Clay Adams) was inserted from the urethra to record UPP. UPP test methods have been described in detail in our previous study [10]. In brief, the bladder was infused with physiological saline at a rate of 0.04 mL/min to the threshold volume (0.4-1mL), which induced isovolumetric rhythmic contractions. The urethral catheter was continuously infused with physiological saline at a rate of 0.04 mL/min. PowerLab (AD Instruments) was used for data acquisition and manipulation. When the rhythmic bladder contractions stabilized for at least 30 min, the maximum amplitude of isovolumetric contractions and the intravesical pressure threshold for inducing urethral relaxation were measured. The following parameters were measured: UPP nadir, the lowest pressure during reflex urethral relaxation; Baseline UPP, mean pressure over 30 min without an increase in intravesical pressure induced by the micturition reflex. UPP change was calculated as baseline UPP minus UPP nadir.

In vitro functional studies with organ bath test on the contractile force of the bladder and urethra

The contractile forces of the bladder and urethra muscle strips were performed by using organ bath (n=6 per group). Organ bath test methods have been described in detail in our previous study [11]. In brief, rats were euthanized in a CO₂ chamber followed by

cervical dislocation. Bladder and urethra were dissected free as a block and immersed in a petri dish containing Krebs-Henseleit solution [containing (in mM) 117 NaCl, 4.7 KCl, 2.5 CaCl₂, 1.2 MgSO₄, 1.2 KH₂PO₄, 25 NaHCO₃, and 11glucose]. Each strip was equilibrated unstretched for 30 min. A load of 1.0 g was applied to each strip by micrometer adjustment, and the load was readjusted to this level 30 min later. Changes in the tone of the strips were measured isometrically using force transducers, and the data were recorded using the Chart v3.6.9 software and the PowerLab/16sp data acquisition system (AD Instruments).

Electrical-field stimulation (EFS) was applied to the isolated bladder and urethral rings placed between two platinum electrodes (1 mm diameter) connected to a Grass S88 stimulator (Astro-Med Industrial Park), respectively. Frequency-response curves (1-32 Hz) were elicited by stimulating the tissues for 10 s with pulse of 1 ms width at 50 V and 2 min intervals between stimulations. After tissues were washed three times, bladder muscle strips were used to examine the cumulative concentration-response curves to the contractile agonist Carbachol (1nM to 100 μM) stimulation. Contraction was produced using a single concentration of KCL (80 mM) in urethral muscle strips. Bladder and urethral contractions were completely abolished by prior incubation with a voltage-gated sodium channel blocker, tetrodotoxin (TTX, 1 μM), confirming the neurogenic nature of responses. Contraction response data were normalized to the wet weight of the respective urethral ring. Cumulative concentration response curves to carbachol in the bladder muscle strips were constructed, and contractile forces to 80 mM of KCL in the urethral muscle strips were also measured.

Haematoxylin & Eosin and Masson's staining in bladder and urethra

The rats were killed with an overdose of pentobarbital (100 mg/kg, sigma, USA), and were transcardially perfused with 4% paraformaldehyde. The entire bladder and urethra were then removed. Transverse 8-μm sections of the collected segments were cut by a freezing microtome and mounted on slides. Every 10th section from the bladder and urethra of each NC and DM rat were subsequently stained with haematoxylin and eosin (H&E) and Masson.

For H&E staining, the slides were immersed in hematoxylin at RT for 30 s, rinsed with running water until transparent, stained with eosin at RT for 30 s and then rinsed again with water. The slides were then air-dried at RT. Subsequently, the slides were sequentially immersed twice in 95% ethanol solution, twice in 100% ethanol, twice in a solution of 50%

ethanol and 50% xylene and twice in 100% xylene. The slides were then observed under a light microscope (Olympus Corporation).

For Masson's staining, the staining process was as follows: (1) Deparaffinize sections if necessary and hydrate in distilled water. (2) Preheat Bouin's Fluid in a water bath to 56-64°C in a fume hood or very well ventilated area. (3) Place slide in preheated Bouin's Fluid for 60 minutes followed by a 10 minutes cooling period. (4) Rinse slide in tap water until section is completely clear. (5) Rinse once in distilled water. (6) Mix equal parts of Weigert's (A) and Weigert's (B) and stain slide with working Weigert's Iron Hematoxylin for 5 minutes. (7) Rinse slide in running tap water for 2 minutes. (8) Apply Biebrich Scarlet / Acid Fuchsin Solution to slide for 15 minutes. (9) Rinse slide in distilled water. (10) Differentiate in Phosphomolybdic / Phosphotungstic Acid Solution for 10-15 minutes or until collagen is not red. (11) Without rinsing, apply Aniline Blue Solution to slide for 5-10 minutes. (12) Rinse slide in distilled water. (13) Apply Acetic Acid Solution (1%) to slide for 3-5 minutes. (14) Dehydrate very quickly in 2 changes of 95% Alcohol, followed by 2 changes of Absolute Alcohol. (15) Clear in Xylene or Xylene Substitute and mount in synthetic resin. Finally, the sections were sealed with neutral gum. Blue collagen fibers, red muscle fibers, red cellulose and red blood cells were observed under a microscope (Olympus Corporation).

Statistics Analysis

All data are expressed using mean and standard error (mean \pm SE). GraphPad Prism software (ver. 6.01, Inc., CA, USA) was used for statistical analysis. One-way or two-way ANOVA followed by Dunnett's multiple comparisons test were used, or Student's t-test was used to assess the results. A P-value < 0.05 was considered significant.

Results

Metabolic cage study

As is shown in Fig. 1, DM and DI groups exhibited a significant increase in 12-h urine volume, urinary frequency/12 hours and voided volume at each point. Moreover, 4 and 8-DM groups had a significant increase in 12-h urine volume and voided volume than 4 and 8-DI group, respectively. In normal control (NC), 4-DI, 4-DM, 8-DI and 8-DM groups of rats, urinary frequency/12 hours were 7.4 ± 0.9 , 19.6 ± 3.4 , 23.2 ± 3.4 , 13.8 ± 3.0 and 18.0 ± 5.4 , respectively. 12-h urine volume was 2.4 ± 1.2 , 37.1 ± 9.3 , 65.7 ± 3.7 , 20.7 ± 9.2 and 47.3 ± 7.2 (mL), respectively. VV was 0.3 ± 0.1 , 1.9 ± 0.3 , 2.9 ± 0.3 , 1.5 ± 0.5 and 2.8 ± 0.9 (mL), respectively.

In vivo functional studies with cystometry and EUS-EMG with open urethra

Normal control rats (n=5). Fig.2 shows typical CMG and EUS-EMG recordings acquired from urethane anaesthetized rats. In the NC group, bladder capacity was 0.58 ± 0.04 ml, VV was 0.53 ± 0.03 ml, VE was $91.05 \pm 1.73\%$, $P_{ves_{max}}$ was 40.78 ± 0.77 cmH₂O, ICI was 5.84 ± 0.43 min, EUS activity duration was 4.28 ± 0.25 s and EUS activity bursting activity was 2.66 ± 0.16 s as shown in Fig. 2.

DM and insulin-treated DM animal models (n=5 per group). As is shown in Fig. 3, typical CMG and EUS-EMG showed longer ICIs, EUS activity duration and EUS bursting activity duration in 4-DM group compared to the NC groups. Bladder capacity, VV and ICI have a significant increase in DM and DI groups; VE and EUS bursting activity duration in 8-DM group were significant lower compared to the NC group. However, no significant difference was observed in $P_{ves_{max}}$ among those groups. Additionally, bladder compliance was significant higher in 4 & 8-DM groups and the 8-DI group compared to the NC group.

Changes in UPP parameters under isovolumetric conditions in DM and insulin-treated DM rats

As is shown in Fig. 4, in NC, 4-DI, 4-DM, 8-DI and 8-DM groups of rats, the value of UPP nadir were 18.20 ± 1.68 , 16.66 ± 1.49 , 21.01 ± 1.28 , 20.07 ± 1.72 , 20.36 ± 1.53 (cmH₂O), respectively; the value of baseline UPP were 34.40 ± 1.36 , 29.85 ± 0.33 , 32.30 ± 1.60 , 33.84 ± 2.25 , 28.28 ± 1.54 (cmH₂O), respectively; the value of UPP change were 16.20 ± 1.40 , 13.19 ± 1.30 , 11.28 ± 0.94 , 13.78 ± 2.79 and 7.93 ± 1.14 (cmH₂O), respectively. Histograms showed that there was no significant difference in UPP nadir and baseline UPP among the groups (Fig. 4 A, B), whereas UPP changes in the 8-DM group were significantly lower than the NC group (Fig. 4 C), indicating that impaired urethral relaxation during voiding exists in the 8-DM group.

In vitro functional studies with organ bath test on the contractile force of the bladder and urethra

In a separated set of experiments, EFS (1-32Hz) induced frequency-dependent contractions in bladder strips from all the groups. After EFS stimulation, bladder contractions were significantly higher in 4 and 8-DM groups compared to the NC group at the frequencies of 16 and 32Hz (Fig. 5A). However, maximum bladder muscle contraction per gram of the tissue to EFS stimulation was significantly lower in 4 and 8-DM group compared to the NC group at the frequencies of 16 and 32 Hz (Fig. 5 B). Moreover,

concentration-response curves were generated to assess the contraction profile in response to muscarinic receptor activation using carbachol (1nM-100 μM) across the different groups. Fig. 6 shows that the bladder contractions to carbachol stimulation in 4 and 8-DM groups were larger than 4 & 8-DI and NC groups (Fig. 6A, B). However, the contractions per milligram of bladder smooth muscle to carbachol were significantly decreased in 4 and 8-DM groups compared to the NC group (Fig. 6 C).

After EFS (1-32HZ) stimulation, the maximum urethral contraction and maximum urethral contraction per gram of the tissue to EFS stimulation were increased in 4 and 8-DM groups compared to the NC group, especially at the frequency of 16 and 32 Hz (Fig. 5C, D). Additionally, maximum urethral contraction and to maximum urethral contraction per

gram of the tissue to KCL stimulation were significantly increased in 4 and 8-DM group compared to the NC group (Fig. 6D, E).

H&E and Masson’s staining

H&E and Masson’s staining showed that DM caused hypertrophic changes in the bladder detrusor muscle with the time-dependent progress in DI and DM groups. Histogram data revealed that the bladder muscle thickness was significantly increased compared to the NC groups in 4 & 8-DM groups and the 8-DI group (Fig. 7A), whereas the ratio of muscle and collagen was not significantly changed in any of the groups (Fig. 7B). Additionally, no significant difference of the urethral muscle thickness and the ratio of muscle and collagen were observed among the groups (Fig. 7C, D).

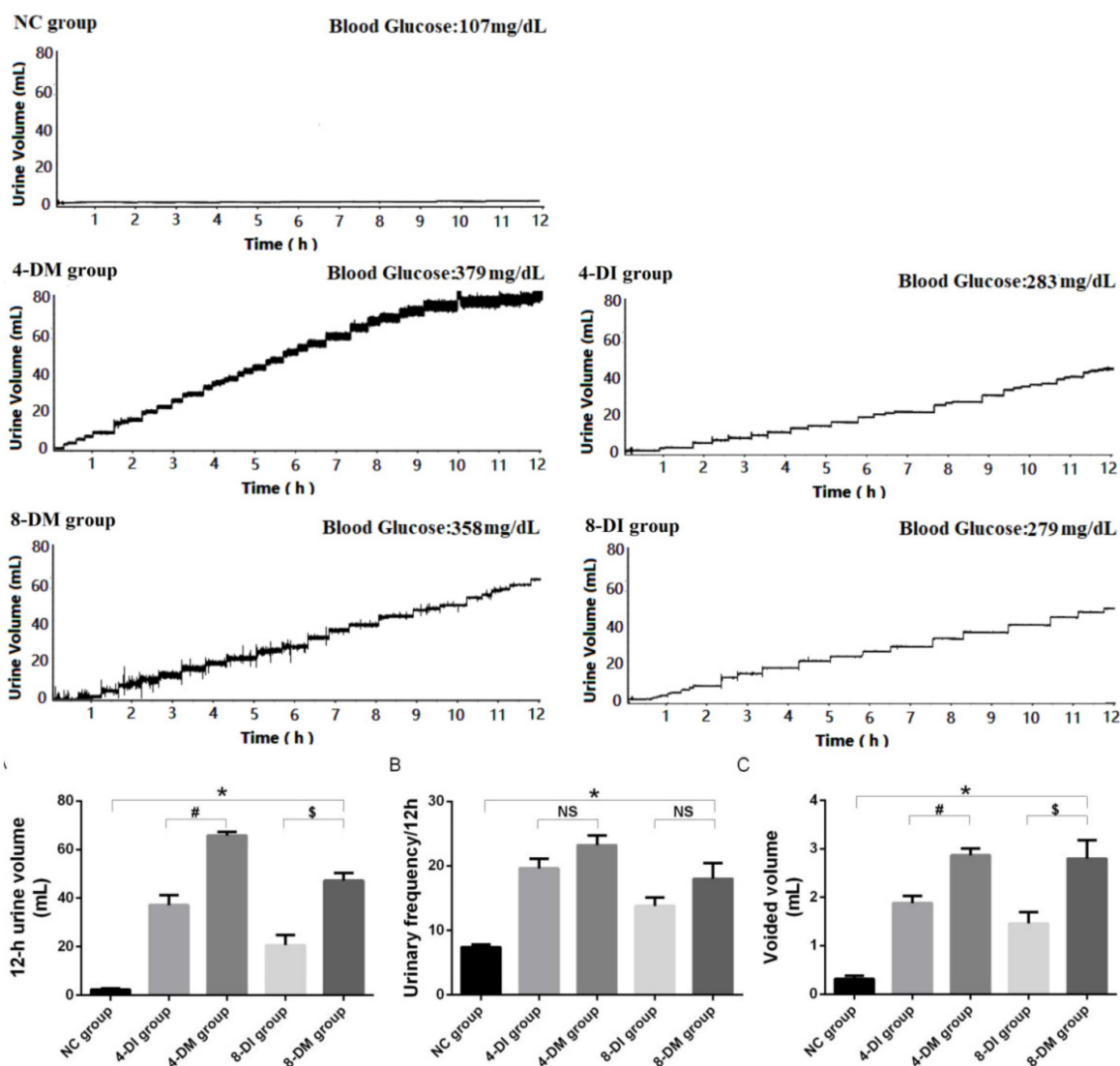


Figure 1. Voiding patterns in metabolic cage study. Diabetes mellitus (DM) and insulin-treated DM groups exhibited an increase in 12-h urine volume, urinary frequency/12 h and voided volume compared to normal control (NC) rats. The 4- and 8-weeks insulin-treated DM group showed the significant smaller values in 12-h urine volume and voided volume compared to the 4- and 8-weeks DM group, respectively. *P < 0.05 compared to the NC group, #P < 0.05 compared to the 4 weeks insulin-treated DM group, \$ P < 0.05 compared to the 8 weeks insulin-treated DM group.

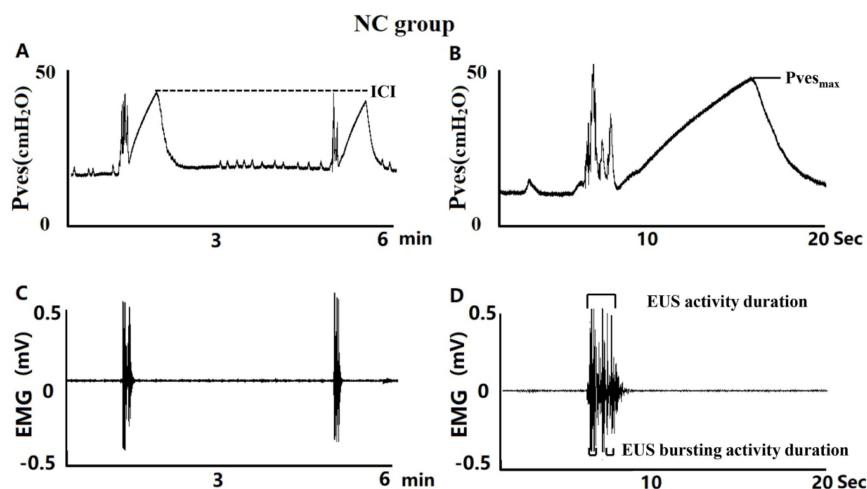


Figure 2. The typical pattern of the intravesical pressure (top trace) and EUS-EMG activity (bottom trace), recorded during a continuous transvesical infusion CMG measurement in a urethane-anesthetized normal control (NC) rat. B and D are traces at an expanded time scale of A and C, respectively. Tonic EUS-EMG activity preceded the large rise in intravesical pressure and shifted to a bursting pattern at the peak of the bladder contraction before the onset of voiding. ICI, intercontraction interval; Pves_{max}, maximal intravesical pressure, is not identical with the micturition pressure, and the true micturition pressure is the pressure at which fluid starts to flow.

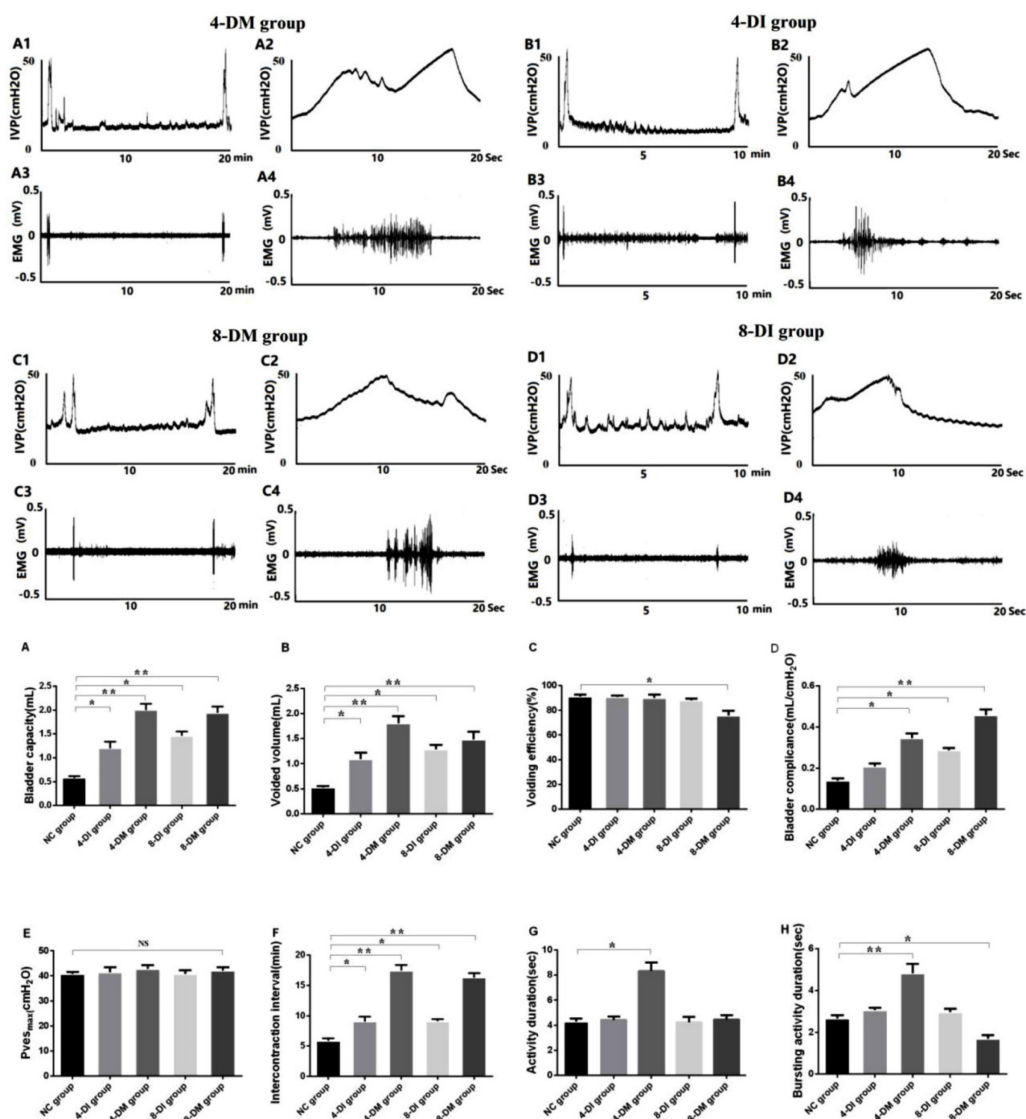


Figure 3. Representative traces showing CMG and EUS-EMG activity in urethane-anesthetized DM and insulin-treated rats. It is clear that ICI was increased in DM rats, and the EUS bursting activity duration was increased in 4 weeks DM rats, but decreased in 8 weeks DM rats. Histograms show that bladder capacity and voided volume were significantly increased in DM and DI groups, whereas voiding efficiency was significantly decreased in the 8 weeks DM group. No significant difference in Pves_{max} was observed in all those groups. *P< 0.05, **P<0.01 vs. corresponding NC group.

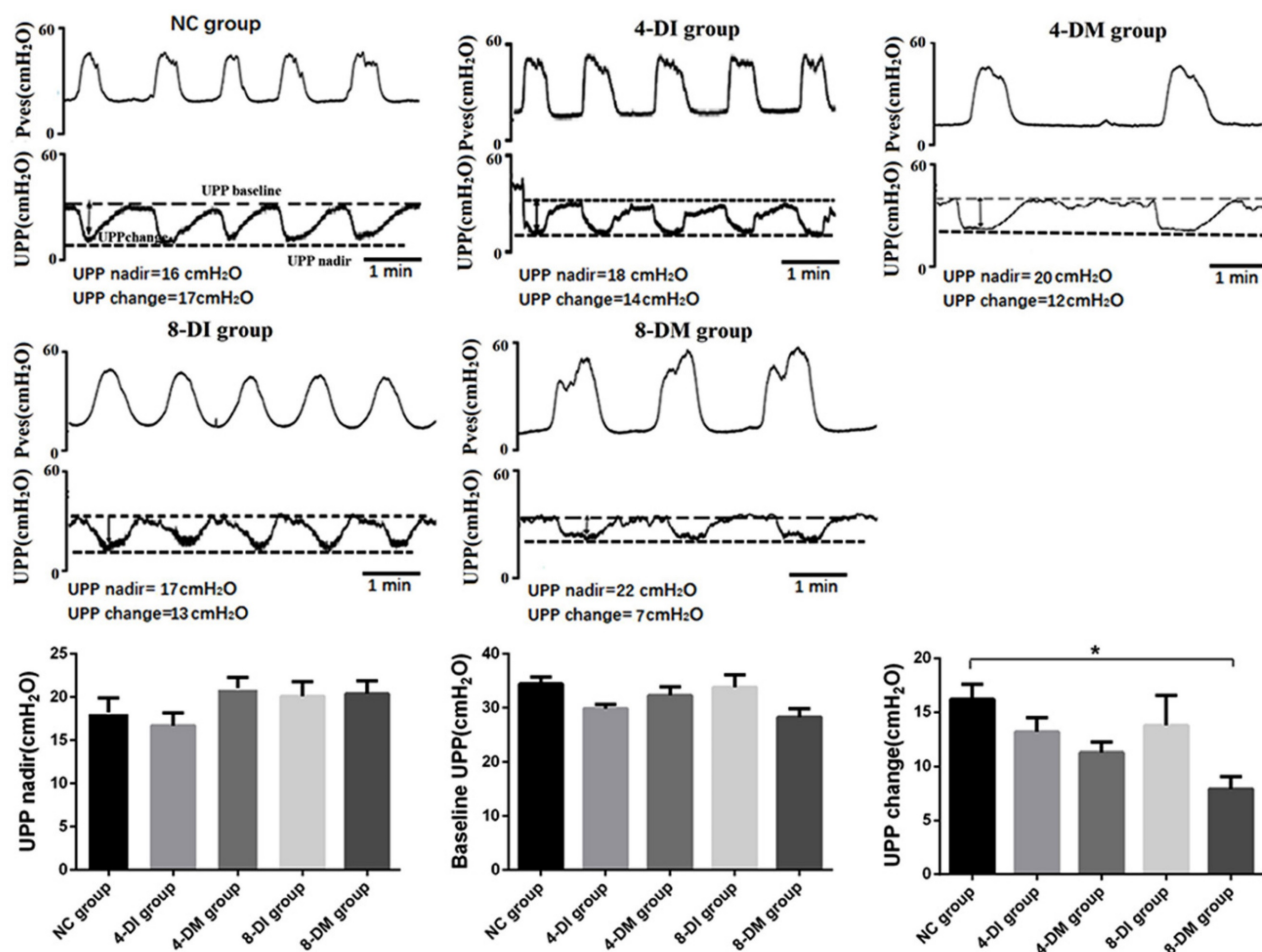


Figure 4. Representative traces showing various parameters in simultaneous recordings of intravesical pressure under the isovolumetric condition and UPP in urethane-anesthetized rats. Histograms of UPP changes shows an obviously decrease in the 8 weeks DM group (C). UPP, urethral perfusion pressure; UPP change, UPP baseline minus UPP nadir. *P < 0.05, vs. corresponding NC group.

Discussions

Diabetes mellitus is a metabolic disorder caused by an absolute or relative deficiency of insulin, which is a debilitating and costly disease with multiple serious complications. Lower urinary tract dysfunction (LUTD) is among the most common complications of DM [15]. Although STZ-induced DM rats have been widely used as a rodent model for LUTD, this is an acutely-induced, severe DM model with high glucose levels that can easily damage other systems in a short period, often leading to early animal death. Hence, this STZ-induced DM model may not be suitable for studying the pathophysiological condition encountered in DM patients, especially those with type 2 DM that is induced by insufficient insulin production and insulin resistance. DM causes the increases in drinking and voiding volume in the early stage, which may be due to the hyperglycemia-induced osmotic polyuria [12]. As the course of the disease progressed, bladder and

urethral function could be damaged by DM, leading to LUTD. Our and other studies have shown the time-dependent alteration of bladder and urethral function in diabetic rats [7, 12], whereas time-dependent changes of LUT function in low-dose insulin-treated DM were not established in previous studies. The current study confirms that diabetic rats have altered micturition patterns, which varied at different time points, including alterations in voided volume, micturition episodes/12 hours and voided volume per micturition (Fig.1). DM and DI groups exhibited a significant increase in 12-h urine volume, urinary frequency/12 hours and voided volume at each point, and 4 and 8-DM group had a significant increase in 12-h urine volume and VV compared to 4 and 8-DI group, respectively. These results demonstrate that the low-dose insulin-treated DM rat is a stable animal model, which can be reliably used for the long-term study of DM-induced bladder and urethral dysfunction.

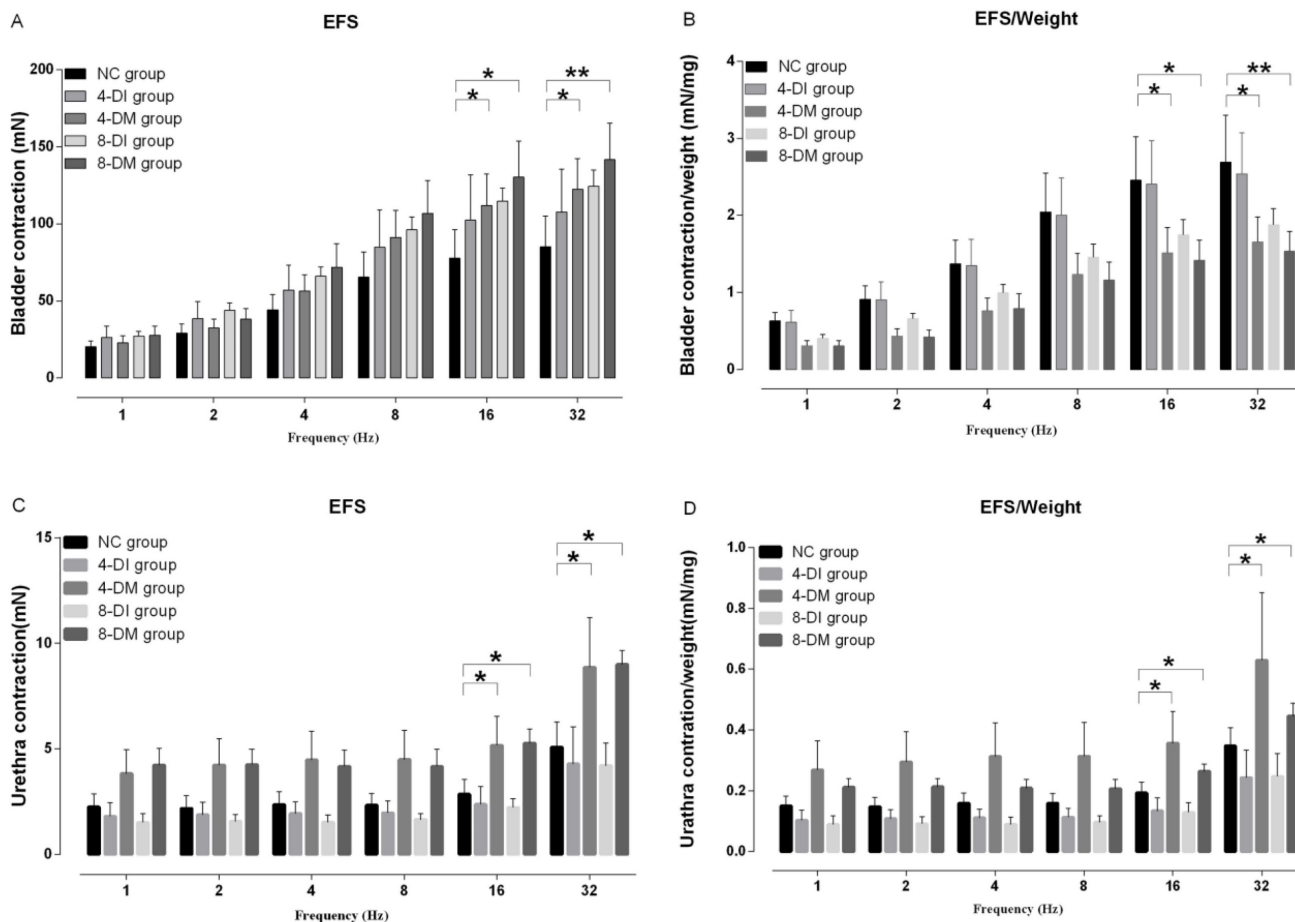


Figure 5. Histograms showing the contraction responses to electrical-field stimulation (EFS, 1-32 Hz) in the bladder (A, B) and urethra muscle strips (C, D) from normal control (NC), insulin-treated DM and DM groups. Data represent the mean \pm S.E.M. (n = 6). *P < 0.05, **P < 0.01 when compared to the NC group.

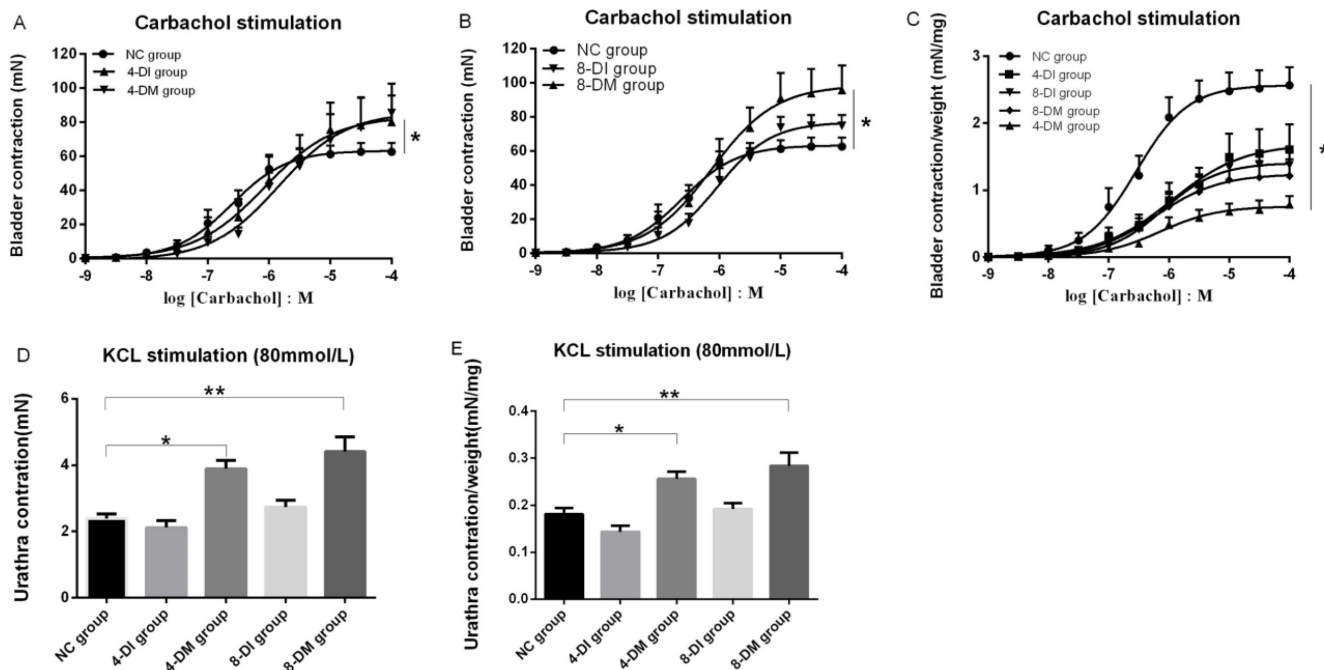


Figure 6. Cumulative concentration-response curves to the contractile agonist Carbachol (1nM to 100 μ M) stimulation in bladder strips (A-C). Histograms show the urethral contraction in response to KCL (80mM) stimulation (D, E), *P < 0.05, **P < 0.01 when compared to the NC group.

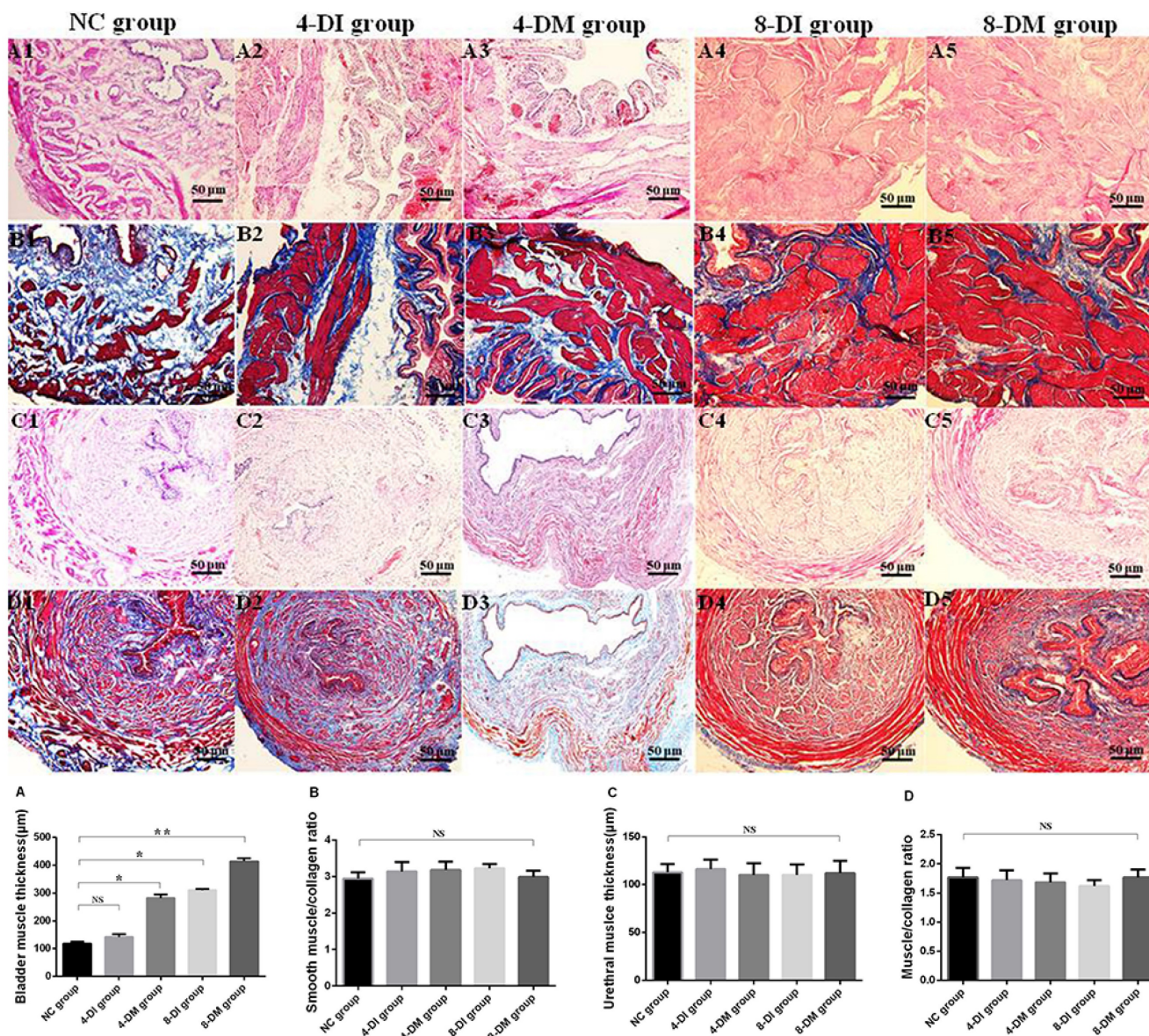


Figure 7. Representative photomicrographs of haematoxylin and eosin (H&E) and Masson’s staining (muscle: red) of bladder in normal control (NC), diabetes mellitus (DM) and insulin-treated DM rats (n=5 per group). (A1-A5) and (C1-C5) were original magnification using H&E staining (40x). (B1-B5) and (D1-D5) were original magnification (40 x) with Masson’s staining. Histograms show the hypertrophic changes in the bladder detrusor muscles in DM rats, whereas urethral muscle layer thickness showed no significant difference in DM groups compared to the NC rat. *P < 0.05 vs corresponding NC group. Scale bar, 50µm.

DM-induced bladder dysfunction (DBD) has been widely reported in STZ-induced animal model. The progress of DBD has been defined as two states, compensatory and decompensatory bladder. The compensatory state that occurs soon after the onset of diabetes, characterized by overactive detrusor, enhanced contractility, and bladder hypertrophy [12]. Subsequently, decompensation occurs in the late stage of diabetes, characterized by slow urine flow, decreased maximum voiding pressure, and symptoms of urine retention and dysuria [13]. The finding of the current study shows that DM could increase the bladder capacity, VV and inter-contraction interval as early as 4 weeks, and this effect becomes more prominent at 8 weeks (Fig.3A, B, F).

However, a significant decrease in voiding efficiency was observed only in 8 weeks DM (Fig.3C). Moreover, we also observed that ICI and bladder compliance were gradually increased in DI and DM group as time progressed but no significant change was observed in 4 weeks DI group (Fig.3D), suggesting low-dose insulin treatment may slow the emergence of bladder dysfunction induced by diuresis-induced bladder overdistention, in line with our previous study, in which, however, only 8 weeks DM rats were used to assess the DM-induced DBD without EUS-EMG recordings [14].

Although DBD has been widely reported in previous studies, little is known about the time-dependent changes in DM-induced urethral

dysfunction. Because the urethra consists of the external urethral sphincter (EUS) and the smooth muscle sphincter, DM-induced urethral dysfunction is mainly characterized by impaired relaxation of the EUS and smooth muscles. In normal rats, EUS activity can be divided into tonic activity and bursting activity. Tonic activity of the EUS reflects a closure phase of the urethral outlet during urine storage, while bursting activity reflects rhythmic opening and closing of the outlet to produce a pulsatile flow of urine, which is commonly observed in rodents [15]. It is assumed that the DM-induced EUS dysfunction would increase outlet resistance and, consequently, decrease voiding efficiency. In our present study, we observed that EUS bursting activity duration was significantly increased in 4-DM group, whereas decreased in 8-DM group, which may suggest that DM-induced EUS dysfunction may be varied from overactivity to underactivity as time progress. Moreover, there were no significant changes of EUS bursting activity in DI groups, indicating that low-dose insulin may slow the progress and protect against the EUS dysfunction.

Furthermore, *in vivo* functional study with UPP recordings, the results found that UPP change significantly decreased in the 8-DM group, which suggested that DM could induce urethral relaxation dysfunction after 8 weeks DM, whereas low-dose insulin could protect against impaired urethral relaxation during voiding. In *in vitro* organ bath study, we found that bladder smooth muscle strips contractions normalized against tissue weight in response to EFS and carbachol stimulation have significantly decreased in DM groups, but not in DI and normal rats. These results suggest that M_2 and M_3 muscarinic receptors are possibly downregulated in the urothelium of the STZ-induced diabetic rats as activation of M_2 and M_3 receptors in the urothelium reportedly increases sensory nerve activity to facilitate the detrusor contraction [16]. Also, we also examine urethra contractions to EFS and KCL stimulation. Urethral smooth muscle strips contractions normalized against tissue weight in response to EFS and KCL stimulation have been increased in DM groups, but not in DI vs. normal rats. These results may be ascribed to the upregulation of α_1 -adrenergic receptors in the urethral smooth muscle of STZ-induced diabetic rats [17, 18]. Also, an increase of ATP-sensitive potassium channel in the urothelium also can increase sensory nerve activity to facilitate urethral muscle contraction [19]. Furthermore, the results from H&E and Masson's staining revealed a progressive increase in the thickness of the bladder smooth muscle layer in 8-DI and 4 & 8-DM groups over time. However, the thickness of the urethral

muscle layer did not show significant changes among the groups. Taken together, it is likely that DM-induced LUTD is time-dependent and include decreased bladder contractility evident as reduced muscle strip contraction per tissue weight (4 & 8-DM rats) and reduced urethral relaxation evident as lower UPP reduction (8-DM rats) and enhanced urethral contraction upon KCL or EFS stimulation (4 & 8-DM rats). Also, the results of this study indicate that DM induces bladder structural remodeling that can be delayed by low-dose insulin treatment as the bladder wall thickness was found in both 4 and 8-DM rats, but only in 8-DI rats, possibly due to a protective effect against osmotic polyuria.

Based on the above findings, the use of sustained-release low-dose insulin injections can create a relatively stable model of DM-induced LUTD. Moreover, low-dose insulin demonstrates a certain protective effect against lower urinary tract dysfunction, potentially mediated through its interaction with insulin receptors in the lower urinary tract [20]. However, it is important to note that low-dose insulin cannot fully reverse the damage caused by diabetes. This may be attributed to other underlying mechanisms, as the pathophysiology of lower urinary tract dysfunction in diabetes involves not only osmotic diuresis but also oxidative stress, inflammation, and other mechanisms [21]. Further research is needed to explore these mechanisms in depth.

There are some limitations in this study. Firstly, we did not use neuromuscular blocking agents such as α -bungarotoxin to separate the smooth and striated muscle activity of the urethra, and therefore EFS-induced transient contraction in urethral ring tissues may be related to EUS contractions. Secondly, UPP recordings were performed under urethane anesthesia, which might not reflect true functionality in the conscious condition. Thirdly, we did not assess the longer effects of the insulin treatment in DM and molecular mechanisms underlying DM-induced changes in the bladder and urethra. Thus, further studies will be planned to clarify these points in the future.

Conclusions

DM-induced LUTD is characterized by the time-dependent functional and structural remodeling in the bladder and urethra, which shows the hypertrophy of the bladder smooth muscle, impaired urethral smooth muscle relaxation and EUS dysfunction. Low-dose insulin can protect against diuresis-induced bladder overdistention and preserve urethral relaxation; however but the longer effects of DM with or without low-dose insulin and molecular

mechanisms underlying DM-induced LUTD should be further explored.

Acknowledgements

This work was sponsored by Shanghai Sailing Program (Grant No. 21YF1434400), the Youth cultivation project of Shanghai Jiao Tong University Affiliated Sixth People's Hospital (Grant No. ynqn202112).

Competing Interests

The authors have declared that no competing interest exists.

References

1. de Groat WC, Griffiths D, Yoshimura N. Neural control of the lower urinary tract. *Comprehensive Physiology*. 2015; 5(1):327-396.
2. Jian F, Pan H, Zhang Z, et al. Sphincter electromyography in diabetes mellitus and multiple system atrophy. *Neurourology and urodynamics*. 2015; 34(7): 669-674.
3. Daneshgari F, Liu G, Hanna-Mitchell AT. Path of translational discovery of urological complications of obesity and diabetes. *American journal of physiology Renal physiology*. 2017; 312(5): F887-F896.
4. Torimoto K, Fraser MO, Hirao Y, et al. Urethral dysfunction in diabetic rats. *The Journal of urology*. 2004; 171(5): 1959-1964.
5. Yang Z, Dolber PC, Fraser MO. Diabetic urethropathy compounds the effects of diabetic cystopathy. *The Journal of urology*. 2007; 178(5): 2213-2219.
6. Daneshgari F, Liu G, Birder L, et al. Diabetic bladder dysfunction: current translational knowledge. *The Journal of urology*. 2009; 182(6 Suppl): 518-26.
7. Cao N, Gu B, Gotoh D, et al. Time-Dependent Changes of Urethral Function in Diabetes Mellitus: A Review. *International neurourology journal*. 2019; 23(2): 91-99.
8. Nakagawa T, Akimoto N, Hakozaiki A, et al. Responsiveness of lumbosacral superficial dorsal horn neurons during the voiding reflex and functional loss of spinal urethral-responsive neurons in streptozotocin-induced diabetic rats. *Neurourology and urodynamics*. 2020; 39(1): 144-157.
9. Kullmann FA, Wells GI, McKenna D, et al. Excitatory effects of bombesin receptors in urinary tract of normal and diabetic rats *in vivo*. *Life sciences*. 2014; 100(1): 35-44.
10. Cao N, Alexandre EC, Gotoh D, et al. Urethral dysfunction and alterations of nitric oxide mechanisms in streptozotocin-induced diabetic rats with or without low-dose insulin treatment. *Life sciences*. 2020; 249: 117537.
11. Alexandre EC, Cao N, Mizoguchi S, et al. Urethral dysfunction in a rat model of chemically induced prostatic inflammation: potential involvement of the MRP5 pump. *American journal of physiology Renal physiology*. 2020; 318(3): F754-F762.
12. Daneshgari F, Liu G, Imrey PB. Time dependent changes in diabetic cystopathy in rats include compensated and decompensated bladder function. *The Journal of urology*. 2006; 176(1): 380-386.
13. Daneshgari F, Huang X, Liu G, et al. Temporal differences in bladder dysfunction caused by diabetes, diuresis, and treated diabetes in mice. *American journal of physiology Regulatory, integrative and comparative physiology*. 2006; 290(6): R1728-1735.
14. Gotoh D, Cao N, Alexandre EC, et al. Effects of low-dose insulin or a soluble guanylate cyclase activator on lower urinary tract dysfunction in streptozotocin-induced diabetic rats. *Life sciences*. 2021; 286: 120001.
15. Kakizaki H, Fraser MO, De Groat WC. Reflex pathways controlling urethral striated and smooth muscle function in the male rat. *The American journal of physiology*. 1997; 272(5 Pt 2): R1647-1656.
16. Pinna C, Zanardo R, Puglisi L. Prostaglandin-release impairment in the bladder epithelium of streptozotocin-induced diabetic rats. *European journal of pharmacology*. 2000; 388(3): 267-273.
17. Torimoto K, Hirao Y, Matsuyoshi H, et al. alpha1-Adrenergic mechanism in diabetic urethral dysfunction in rats. *The Journal of urology*. 2005; 173(3): 1027-1032.
18. Chen S, Zhu Y, Feng X, et al. Changes in alpha1-adrenoceptor and NGF/proNGF pathway: a possible mechanism in diabetic urethral dysfunction. *Urologia internationalis*. 2014; 93(3): 344-351.
19. Ohmasa F, Saito M, Shimizu S, et al. The role of ATP-sensitive potassium channel on acute urinary retention and subsequent catheterization in the rat. *European journal of pharmacology*. 2010; 635(1-3): 194-197.
20. Chen H, Wu A, Zeidel ML, et al. Smooth Muscle Insulin Receptor Deletion Causes Voiding Dysfunction: A Mechanism for Diabetic Bladder Dysfunction. *Diabetes*. 2022; 71(10): 2197-2208.
21. Yuan Z, Tang Z, He C, et al. Diabetic cystopathy: A review. *J Diabetes*. 2015; 7(4): 442-447.